Contribution to the study of the transition to a superstructure in high yttria content YCSZ[☆]

Angela Gallardo-López, Julián Martínez-Fernández, Arturo Domínguez-Rodríguez*

Departamento de Física de la Materia Condensada, Universidad de Sevilla, Apdo. 1065, 41080 Sevilla, Spain

Abstract

This work deals with the interpretation of the diffuse spot array observed in experimental electron diffraction patterns (DPs) of 24–32 mol% yttria completely stabilized zirconia (YCSZ). DPs corresponding to the microdomains of $Y_4Zr_3O_{12}$ compound described as an hexagonal structure in a cubic fluorite matrix have been simulated, paying special attention to the relationship between the cubic and the hexagonal structures. The comparison between experimental and simulated electron DPs has been used to test the proposed model of microdomains of δ-phase forming in the cubic fluorite matrix as an explanation to the phenomenon of diffuse scattering. © 2002 Elsevier Science Ltd. All rights reserved.

Keywords: Domains; Electron diffraction; Electron microscopy; Superstructure; ZrO_2

1. Introduction

In a previous work Gallardo-López et al.[1] dealt with the problem of the diffuse scattering distribution found experimentally in electron diffraction patterns (DPs) of several zone axis: $<112>_c$, $<110>_c$ and $<111>_c$ of the cubic YCSZ, in the range of 24–32 mol% yttria. Different causes for this observations were then discussed, but the experimental array of diffuse spots suggested that different superstructures could form within the matrix and produce extra spots, which, due to the incipient stage of the new superstructure would be diffuse. A microdomain explanation for the diffuse scattering, supported by previous works for the defective fluorite-type phases[2,3] was considered. Based on the literature, three compounds were possible candidates to test this hypothesis:

a) a cubic pyrochlore-type structure corresponding to $Y_2Zr_2O_7$;[4]
b) a cubic c-type binary oxide, yttria: Y_2O_3;[5]
c) a rhombohedral "δ-phase" structure: $Y_4Zr_3O_{12}$.[6]

This latter compound has been detected in the system ZrO_2–Y_2O_3 for high yttria concentrations (40 mol%), as it can be seen in the phase diagram.[7]

In this work we treat in detail the simulation of the diffraction patterns of the structure $Y_4Zr_3O_{12}$ with the purpose of comparing them with the experimental ones. For that reason, we describe carefully the transformation between the different crystal structures of the matrix (cubic YCSZ) and the delta phase (rhombohedral described in terms of hexagonal axes). Making use of the transformation matrices between both structures, we show the equivalent zone axes for the fluorite and for $Y_4Zr_3O_{12}$, and we optimize the more suitable ones for superposition between experimental and simulated diffraction patterns. The results of this comparison are fundamental for the interpretation of the diffuse diffraction patterns of YCSZ.

2. Experimental procedure

The comparison between the yttria or pyrochlore structures and the fluorite matrix in terms of DPs is rather straight-forward because all of them are cubic structures. We assume for simplicity two facts: (a) matrix and precipitate are coherent and (b) the orientation of both structures is the same. To find out whether the experimental diffuse features in a DP are caused by one

---

of these cubic superstructures we have to check out if the diffuse array can be reproduced by the DP of the superstructure. This process needs to be carried out in the main zone axis of each structure, repeating the procedure for different zone axes. However, the comparison between the non cubic precipitate (being either the rhombohedral δ-phase ($Y_4Zr_3O_{12}$), or its hexagonal representation), in the cubic matrix, requires previously a linear transformation between the structures. Considering this δ-phase more relevant and complicated, we will detail here its relationship with the fluorite structure as a previous step for the interpretation of the diffuse DPs.

The structure of the δ-phase derives from the defective fluorite structure by ordering of oxygen vacancies to produce a rhombohedral cell, whose axis are related to the distorted fluorite and whose volume is 1.75 times that of the fluorite cell. There are two types of cationic positions, one octahedral in the origin, and 6 equivalent sites with coordination 7. Cations can be ordered in different ways, provided the cation with smaller ionic radius occupies the octahedral sites. The octahedral site is only occupied by Zr, while the rest are randomly occupied by Zr and Y in a 1:2 ratio, as required by stoichiometry.

The crystal structure of the particular compound $Y_4Zr_3O_{12}$ was refined by Scott.[6] Its space group has been identified as $R\bar{3}$, and the lattice parameters have been estimated as $a = 0.97345$ nm and $c = 0.91092$ nm when described in terms of hexagonal axes (from now on we will use the hexagonal representation for this structure, in agreement with Ref. 6). This compound is stable up to a temperature of 1382 ± 5 °C, at which it disorders to give the fluorite solid solution.

The experimental observation of the diffuse intensities in the DPs was achieved with great accuracy thanks to a Zeiss TEM operating at 120 kV with an Omega filter for the inelastic scattered electrons. Conventional transmission electron microscopes operating at different voltages (200–300 kV) were also used. The samples for observation in TEM were thinned to electron transparency by conventional methods: polishing with diamond abrasives and final ion-milling with a Gatan.

For the computer simulations of the electron DPs of the δ-phase $Y_4Zr_3O_{12}$, we used the EMS software (Electron Microscope Simulation[8]). This program simulates conventional and high resolution DPs from the crystal model introduced by the user. The crystallographic parameters introduced for the simulation were taken from the structure refinements found in the literature.[4–6]

3. Results and discussion

The diffuse spots and lines found experimentally in the DPs appear brighter and sharper when an Omega filter for inelastically scattered electrons is used, so we will show only filtered pictures. This filter minimizes the diffuse background produced by the inelastic contributions, which allows us to obtain a better picture of the diffuse pattern. The experimental DPs of the material in the main zone axes are shown in Fig. 1a ($<112>_c$), b ($<110>_c$) and c ($<111>_c$). A small area of each DP has been magnified and is shown beside each figure. The spots corresponding to the fluorite reflections are easy to distinguish, since they appear brighter and form real spots. The diffuse scattering follows a rather well defined pattern, concentrating in small areas with different shapes: streaks, spot-like, but not giving well defined and sharp spots. The intensity of the diffuse features varies with the foil orientation, being more easily observed in $<112>_c$ directions (Fig. 1a), and minor in $<100>_c$ (not shown here).

In order to make a simulation of electron DPs of the structure consisting of a fluorite matrix with small precipitates of the rhombohedral (described as hexagonal) δ-phase $Y_4Zr_3O_{12}$, first we simulated the structure $Y_4Zr_3O_{12}$ alone. As a result of this, we obtained different DPs in several zone axis; the next step consists of matching them with the experimental DPs taken in the main cubic zone axes, as shown in Fig. 1. Since a precipitate can form in more than one orientation, we have to look for all the possible variants. We assume that the matrix-precipitate interfacial energy is minimum when the unit cell axes of both structures are parallel (coherent precipitate). The change from the cubic fluorite cell description to the hexagonal cell for finding the equivalent crystallographic planes and directions between YCSZ and $Y_4Zr_3O_{12}$, requires a linear transformation of the vectors of the original cubic base, which change their length and orientation. To simulate DPs systematically, as well as to obtain the different variants which superimpose in a certain zone axis, it is absolutely necessary to express the δ-phase superstructure in terms of the cubic subcell, what is done in the next paragraphs.

We will use the notation given by Ref. 9. If we denote (a, b, c) as the vectors of the cubic base, the new hexagonal basis will be given by:

$$(a', b'c')_h = (a, b, c)_c P \tag{1}$$

where P is the transformation matrix. The covariant magnitudes in this transformation are the Miller indices of a plane or a set of planes ($h\ k\ l$) in the direct space (or the coordinates of a direction $<h\ k\ l>$ in the reciprocal space) so that the following applies:

$$(h', k', l')_h = (h, k, l)_c P \tag{2}$$

In the second hand, the vectors of the basis of the reciprocal space (a^*, b^*, c^*) and their covariant magnitudes,
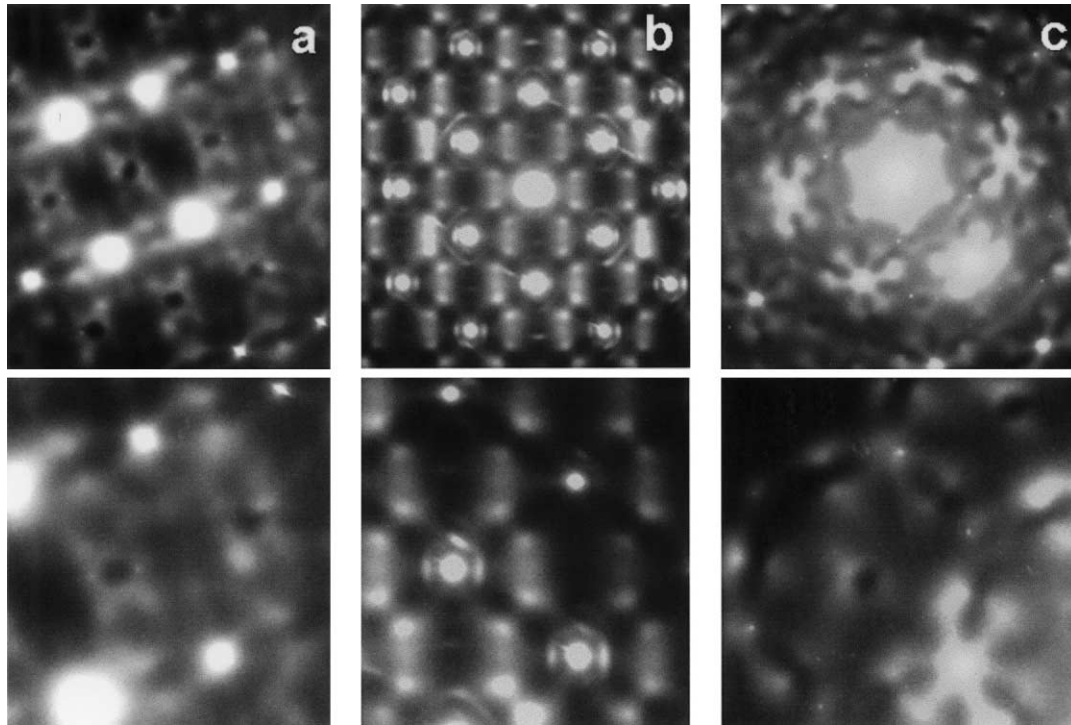
Fig. 1. Experimental DPs of 32 mol% YCSZ in the most significant zone axes where the diffuse scattering was more clearly observed. Besides the strong reflections corresponding to the cubic fluorite structure of YCSZ, we can observe a clear pattern of rather diffuse intensity. The zone axes shown are (a) $<112>_c$, (b) $<110>_c$ and (c) $<111>_c$. Near the figures there is an enlarged area of each one.

the Miller indices of a direction in the direct space $[u\ v\ w]$ use the Q matrix, inverse of P, for the transformation:

$$\begin{pmatrix} a^{*\prime} \\ b^{*\prime} \\ c^{*\prime} \end{pmatrix}_h = Q \begin{pmatrix} a^* \\ b^* \\ c^* \end{pmatrix}_c \tag{3}$$

$$\begin{pmatrix} u' \\ v' \\ w' \end{pmatrix}_h = Q \begin{pmatrix} u \\ v \\ w \end{pmatrix}_c \tag{4}$$

$$Q = P^{-1} \tag{5}$$

The rhombohedral centro-symmetric structure of the δ phase, symmetry $R\bar{3}$, is related to the cubic $Fm\bar{3}m$ with $a_r = a_c \frac{1}{2}\sqrt{2}$ and $\alpha = 60°$ (rhombohedral axes that will not be considered further). Also a face centered cubic cell with reticular parameter a_c can be considered as a triple hexagonal cell with $a_h = a_c \frac{1}{2}\sqrt{2}$ and $c_h = a_c\sqrt{3}$ (hexagonal axes).

Assuming that the δ domains are coherent with the fluorite matrix and the c_h axis thus aligns along $<111>_c$, there are eight possible orientations of the hexagonal supercell of compounds of the type $A_3B_4O_{12}$ in the cubic subcell.[10] Each of the three components of the rhombohedral axis $\vec{a}_R, \vec{b}_R$, and $\vec{c}_R$ and of the hexagonal $\vec{a}_h, \vec{b}_h$ and $\vec{c}_h$ can be expressed in terms of the cubic base, so we can obtain different transformation matrices, P.

Since taking all the P matrices results in redundant information, we only need to use one transformation matrix and calculate all the hexagonal axes corresponding to a set of equivalent cubic zone axes. For instance,[11] we can express the hexagonal axis of the delta phase in terms of the fluorite structure (c) as follows:

$$\vec{a}_\delta = \frac{1}{2}\left[12\bar{3}\right]_c$$

$$\vec{b}_\delta = \frac{1}{2}\left[2\bar{3}1\right]_c$$

$$\vec{c}_\delta = [111]_c \tag{6}$$

the transformation matrices between both structures being P and Q:

$$P = \frac{1}{2}\begin{pmatrix} 1 & 2 & 2 \\ 2 & 3 & 2 \\ 3 & 1 & 2 \end{pmatrix} \tag{7}$$

$$Q = P^{-1} = \frac{1}{21}\begin{pmatrix} \bar{8} & \bar{2} & 10 \\ 10 & 8 & 2 \\ \bar{7} & \bar{7} & \bar{7} \end{pmatrix} \tag{8}$$

Applying these transformations it is possible to obtain the corresponding parallel crystallographic directions of both structures.
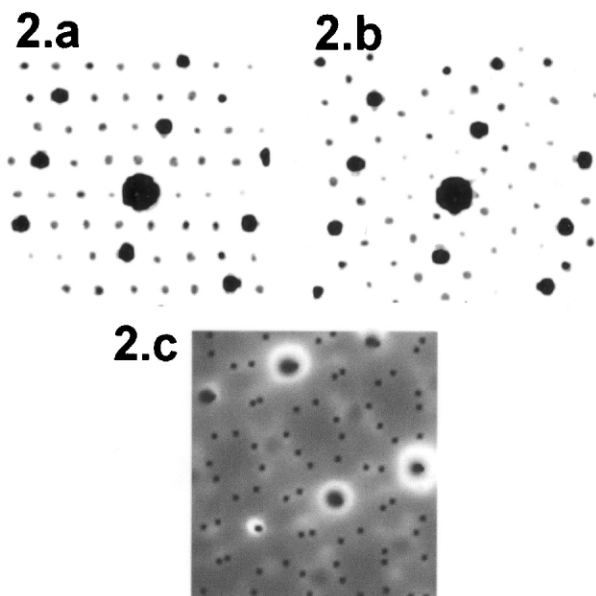
Fig. 2. Simulation of the δ-phase compound $Y_4Zr_3O_{12}$ (hexagonal representation) in (a) $[211]_H$ and (b) $[1\bar{1}\bar{1}]_H$ zone axes. These two hexagonal directions are equivalent to the $[1\bar{1}2]_c$ and $[211]_c$ respectively if we use the transformation described in this work. The strongest reflections of the δ phase coincide with cubic reflections of the fluorite YCSZ in a $<112>_c$ zone axis. In (c) the combination of the simulated DPs (a) and (b) (dark grey spots) is superimposed to the experimental diffuse DP (white spots and white diffuse features).
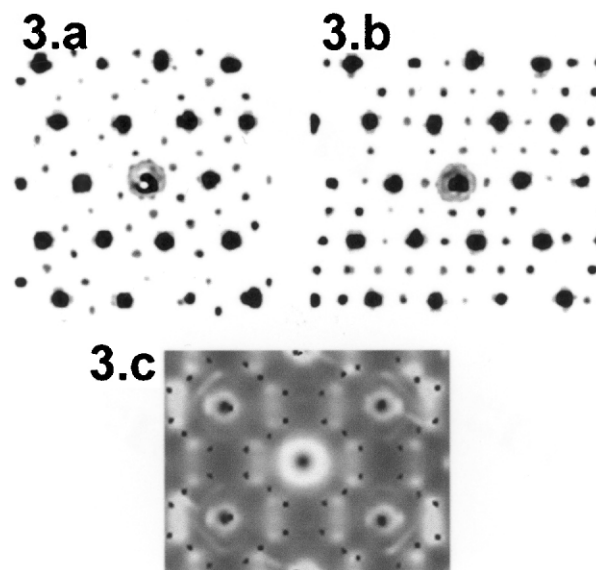

Fig. 3. Simulation of the δ-phase compound $Y_4Zr_3O_{12}$ (hexagonal representation) in (a) $[211]_H$ and (b) $[1\bar{1}\bar{1}]_H$ zone axes. The strongest reflections of the δ phase coincide with cubic reflections of the fluorite YCSZ in a $<110>_c$ zone axis. In (c) the combination of the simulated DPs (a) and (b) (dark grey spots) is superimposed to the experimental DP (white spots and white diffuse features).

We considered the cubic zone axis $<112>_c$, in which the experimental diffuse scattering was clearer and more easily observed. To check all the possible DPs, we represented twelve $<112>_c$ fcc directions: 112, $\bar{1}12$, $1\bar{1}2$, $11\bar{2}$, 121, $\bar{1}21$, $1\bar{2}1$, $12\bar{1}$, 211, $\bar{2}11$, $2\bar{1}1$, $21\bar{1}$, and the equivalent ones for the delta phase structure in hexagonal axis for 8 transformation matrices, obtaining 96 (12×8) zone axes that could superimpose to a cubic $<112>_c$ (even when we knew that the DPs are symmetry related, and some of the directions are redundant). These DPs differ only in their orientation, they can transform into one another by rotation, and some of them are just identical. We chose among them the ones with the lowest indices in order to obtain the largest amount of information from the DPs, and also because they are the most likely zones to appear in the DP. These were:

$$\left[12\bar{1}\right]_h, \left[\bar{1}2\bar{1}\right]_h, \left[1\bar{1}\bar{1}\right]_h, \left[\bar{1}11\right]_h, \left[\bar{2}\bar{1}\bar{1}\right]_h \text{ and } \left[211\right]_h \quad (9)$$

Actually, $[\bar{2}\bar{1}\bar{1}]_h$ gives the same DP than $[1\bar{1}\bar{1}]_h$, and $[211]_h$ gives the same DP as $[\bar{1}11]_h$. The DPs corresponding to opposite sign zone axis transform into one another by means of a mirror reflection. For that reason, the superposition to the cubic DP of just two of these hexagonal variants $[211]_h$ equivalent to $[1\bar{1}2]_c$ and $[1\bar{1}\bar{1}]_h$ equivalent to $[211]_c$ shown in Fig. 2a and b, was enough to reproduce the experimental DPs in $<112>_c$, as can be seen in Fig. 2c, where the simulation is superimposed to the experimental DP of Fig. 1a. The subcell

reflections coincide with the fluorite YCSZ, while the weaker supercell reflections draw a pattern that follows the experimental diffuse scattering.

The simulated DPs for the δ-phase microdomains in the zone axes equivalent to the cubic $<110>_c$ are identical to the DPs of YCSZ. That means that if microdomains and matrix were always coherent, that zone axis would not show extra spots. The experimental observations show that this is not the case. The diffuse scattering is also observed in $<110>_c$ (Fig. 1b) with a particular and well defined pattern, that can be reproduced by $[1\bar{1}\bar{1}]_h$ and $[211]_h$, (Fig. 3a and b) same DPs that could be detected in $[112]_c$. The result of the superposition of simulated and real DPs for this zone axis is shown in Fig. 3c. This is easily understandable if we take into account that according to the transformation used by Rossell and Hanninck[10] between cubic and rhombohedral structures, $<112>_c$ corresponds to $<001>_r$, the highest symmetry zone axis for the rhombohedral δ-phase and the DP of a high symmetry zone axis is always easier to detect. Therefore, this fact points out to a flat or planar shape of the microdomains, rather than a spherical one so the δ-phase will show the same (and most likely) DP in different orientations of the matrix. There should be anyway a preferred orientation of these microdomains to align along $<112>_c$, where the interfacial energy is a minimum, and this is supported by the experimental observations. The diffuse scattering is most clear and easily viewed in the mentioned foil orientation, and the best fit between the experimental and the simulated DPs is also achieved for this foil orientation.
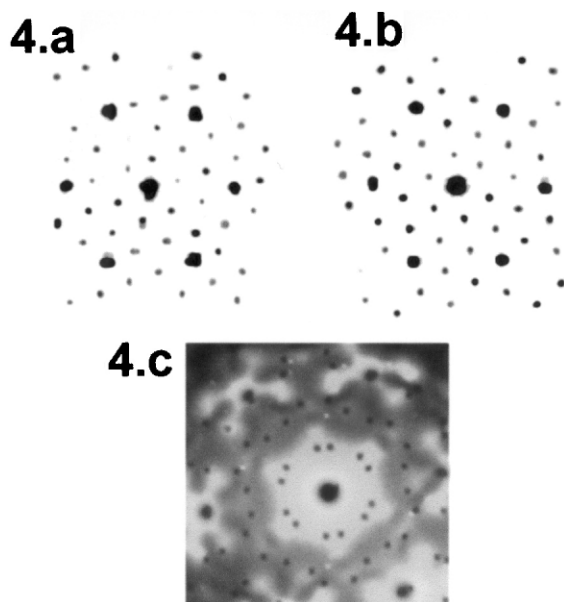
Fig. 4. Simulation of the δ-phase compound $Y_4Zr_3O_{12}$ (hexagonal representation) in (a) $[001]_h$ zone axis, (equivalent to $<111>_c$) and (b) rotated 60°. The strongest reflections of the δ phase correspond to the cubic reflections of the fluorite YCSZ in a $<111>_c$ zone axis. In (c) the combination of the simulated DPs (a) and (b) (dark grey spots) is superimposed to the experimental DP (white spots and white diffuse features).

According to this assumption of planar microdomains in preferred orientations, we used the DPs of Fig. 4a and b, corresponding to a $[001]_h$ to check the experimental array of diffuse spots in $<111>_c$, that we saw in Fig. 1c, the result of this comparison being shown in Fig. 4c.

We need to emphasize that a perfect coincidence between diffuse regions and spots of the δ-phase is not expected, first of all because we are comparing spots with larger areas, since the phase is not completely formed and the microdomains still not grown enough. Secondly, because the diffuse regions may confuse us and make us think that a spot will appear in the center of each of them, which is not usually the case. However, this comparison makes sense when the total pattern can be reproduced by the simulation and when this simulation actually delimitates the diffuse areas, which is our case.

4. Conclusions

The use of a linear transformation between the cubic fluorite structure of YCSZ and the rhombohedral (expressed in hexagonal axes) structure of the delta-phase $Y_4Zr_3O_{12}$ has allowed us to compare successfully DPs of both phases to explain the complex diffuse DP observed experimentally. It has also given us a clue to the most convenient zone axis to study this diffuse phenomenon, the $<112>_c$ equivalent to the hexagonal $[1\bar{1}\bar{1}]_h$ according to the transformation described in this work and also equivalent to the highest symmetry zone

axis for the rhombohedral, $<001>_r$. The assumption of very small microdomains of this delta-phase proves then rather appropriate to interpret the experimental diffuse electron diffraction patterns, based on the agreement of the simulated DPs of the δ-phase and the experimentally observed DPs in this high yttria content YCSZ. This phase is still not completely formed in the material and the microdomains should be rather small in size and oriented preferably along $<112>_c$ zone axis. Their shape should be planar, in view that they present DPs that correspond to $<001>_r$ in several foil orientations of the matrix.

Acknowledgements

References

1. Gallardo-López, A., Martínez-Fernández, J., Domínguez-Rodríguez, A. and Ernst, F., Origin of diffuse electron scattering in YCSZ single crystals with 24 to 32 mol% yttria. *Phil. Mag.* A, 2001, **81**, 1675–1689.
2. Allpress, J. G. and Rosssell, H. J., A microdomain description of defective fluorite-type phases $Ca_xM_{1-x}O_{2-x}$ (M = Zr, Hf; x = 0.1–0.2). *J. Solid State Chem.*, 1975, **15**, 68–78.
3. Rossell, H. J., Ordering in anion-deficient fluorite-related oxides. In *Advances in Ceramics: Science & Technology of Zirconia*, Vol. 3, 1981.
4. Fan, F.-K., Kuznetsov, A. K. and Keler, E. K., Phase Relations in the Y2O3-ZrO2 system: II. *Izv. Akad. Nauk SSSR, Ser Khim.*, 1963, **4**, 601.
5. Paton, M. G. and Maslen, E. N., *A refinement of the crystal structure of yttria. Acta Cryst*, 1965, **19**, 307.
6. Scott, H. G., The yttria-zirconia δ phase. *Acta Cryst.*, 1977, **B33**, 281–283.
7. Yoshimura, M., *Phase stability of zirconia. The Amer. Ceramic. Bull*, 1988, **12**, 1950–1955.
8. Stadelmann, P., & Jouneau, P.H., EMS: Electron microscopy simulation. Centre Interdépartememtal de Microscopie Electronique, EPFL., Laussane (http://cimewww.epfl.ch,® 1995–1999).
9. Hahn, T. (ed.), *International Tables of Crystallography*, Vol. A. Space Group Symmetry. D. Reidel, Dordrecht, The Netherlands/ Boston, USA, 1983.
10. Rossell, H. J. and Hannink, R. H., In *Advances in Ceramics: Science and Technology of Zirconia II*, ed. N. Claussen, M. Rühle and A. Heuer. 1984, pp. 139–151.
11. Yovanovitch, O. and Delamarre, C., Contribution a l'étude de composes de structure derivant de la fluorine dans les systemes ZrO_2-MgO, HfO_2-MgO et HfO_2-Sc_2O_3. *Mat. Res. Bull.*, 1976, **II**, 1005–1010.